Deuterium permeation behavior of zirconium oxide coating after exposure to solid breeder pebbles

Wataru Matsuura [a], Akiyoshi Suzuki [a], Julia Leys [b], Regina Knitter [b], Takumi Chikada [a,*]

[a] Shizuoka University, Shizuoka, Japan
[b] Karlsruhe Institute of Technology, Institute for Applied Materials, Karlsruhe, Germany

ARTICLE INFO

Keywords:
Tritium
Permeation
Ceramics coating
Solid breeder
Corrosion

ABSTRACT

Tritium permeation barrier has been developed using ceramic coatings to mitigate tritium leakage through structural materials in most of the fusion reactor blanket concepts. In a solid breeder blanket concept, corrosion of the coating is a serious issue in addition to tritium permeation; however, the effects of corrosion on tritium permeation have been rarely researched. Here, we report deuterium permeation behaviors of zirconium oxide coatings prepared by metal organic decomposition after exposure to two kinds of solid breeder pebbles with different compositions, followed by deuterium permeation measurements. The deuterium permeation flux varied with the pebble composition: the coated sample after exposure to the pebbles of 30 mol% lithium metatitanate and 70 mol% lithium orthosilicate was smaller than that after exposure to the pebbles of 20 mol% lithium metatitanate and 80 mol% lithium orthosilicate. Because the thickness of the corrosion layer formed by the pebbles with 30 mol% lithium metatitanate and 70 mol% lithium orthosilicate was larger, the composition of the pebbles affected the thickness of the corrosion layer and the permeation behaviors rather than coating integrity.

1. Introduction

In a D-T fusion reactor, tritium will be produced and recovered to establish a self-sufficient fuel cycle. Since hydrogen isotopes including radioactive tritium have high permeability in most metals at operating temperatures, tritium permeation through structural materials is a serious issue in terms of securing an efficient fuel system and radiological safety. Besides, in the solid blanket concepts, corrosion of the structural materials by lithium-containing tritium breeder pebbles is also a concern. To solve these problems, fabrication of a functional coating on the structural materials was proposed, and various kinds of coating materials have been investigated for nearly half a century [1,2]. In our previous study, ceramic coatings such as yttrium oxide, erbium oxide, and zirconium oxide (ZrO_2) coatings showed high permeation reduction performance [3]. Moreover, the compatibility between the coatings and the solid tritium breeder pebbles was also investigated by exposure tests in an environment simulating the solid blanket [4]. After the exposure tests, iron oxides formed from steel substrates, resulting in peeling and degradation of the coating. Although these studies separately investigated hydrogen isotope permeation and corrosion behaviors, there are only a few studies on the combined effects of permeation and corrosion. For the safe operation, the effects of the corrosion by the breeder pebbles on tritium permeation behavior must be clarified. In this study, the deuterium permeation behavior of the ZrO_2 coatings after exposure to two kinds of solid tritium breeder pebbles was investigated to establish the database of tritium permeation in the solid breeder blankets.

2. Experimental details

2.1. Sample preparation

Reduced activation ferritic/martensitic steel F82H (Fe-8Cr-2W, F82H-BA07 heat) plates with dimensions of 25 mm in width, 25 mm in length, and 0.5 mm in thickness were used as substrates. ZrO_2 coatings were fabricated by metal organic decomposition (MOD) as conducted in our previous study [5]. The fabrication process consists of dipping, drying, pre-heating, and heat treatment. First, the F82H substrates were dipped into a metal-organic liquid precursor (SYM-ZR04, Kojundo Chemical Laboratory Co., Ltd.) and withdrawn at a constant speed of 1.0 mm s^{-1}. Second, the sample was dried at 150 °C for 6 min and then pre-heated at 550 °C for 2 min in air using hot plates. The set of dipping,

* Corresponding author.
E-mail address: chikada.takumi@shizuoka.ac.jp (T. Chikada).

Table 1
Composition ratio of solid breeder pebbles.

Pebble	LMT / mol%	LOS / mol%
LMT30	30	70
LMT20	20	80

Table 2
Sample name and annealing parameters.

Sample	Duration / day	Pebble
Z30P16	16	LMT30
Z20P16	16	LMT20
Z30P32	32	LMT30
Z20P32	32	LMT20

drying, and pre-heating was repeated twice. Finally, the sample was heat-treated at 700 °C for 30 min in a quartz tube in a 50 vol% argon-50 vol% hydrogen mixture gas, each with a flow rate of 50 standard cubic centimeters per minute (sccm). The coating thickness was approximately 150 nm. After fabrication, the coated samples were cut into half or quarters for annealing tests with solid breeder pebbles.

2.2. Annealing with solid breeder pebbles

The annealing test under a simulated solid breeder blanket environment is described in detail in Ref. [4]. The solid breeder pebbles consisted of lithium metatitanate (Li_2TiO_3, LMT) and lithium orthosilicate (Li_4SiO_4, LOS) with a dimension of approximately 700 μm in diameter were fabricated by the KALOS process [6]. The composition ratio of the pebbles was 20 mol% LMT-80 mol% LOS and 30 mol% LMT-70 mol% LOS, as shown in Table 1. The coatings were set into alumina boats with the coated side upward, and the pebbles were poured into the alumina boats to cover the coated side of the sample. Detailed information on the annealing equipment is available in Ref. [7]. The alumina boats were annealed in an alumina tube in helium with 0.1 vol% hydrogen purge gas with a flow rate of 1200 ml h^{-1} and a pressure of 1200 mbar. At both the influent and effluent sides, the concentrations of moisture (H_2O) and oxygen (O_2) were monitored. The moisture concentration at the influent side was 90–800 ppm, while that at the effluent side was over 10,000 ppm at the beginning of the test and then decreased to less than 1000 ppm in a day. The oxygen concentrations at the influent and effluent sides were 1900–2100 and 1400–2400 ppm, respectively. The annealing duration was 16 and 32 days, and the test temperature was 550 °C. The samples used in this study are summarized in Table 2.

2.3. Deuterium permeation measurement

Deuterium permeation measurements for the coated samples after the annealing tests were conducted using a gas-driven permeation apparatus. The configurations of the apparatus and the measurement procedure are described in detail in Ref. [8]. The sample was placed in the apparatus with the coated side facing to the D_2-introducing side (upstream). Ion currents of $m/z = 3$ and 4 corresponding to HD and D_2 were detected at the permeated side (downstream) using a quadrupole mass spectrometer (QMS, M-201QA-TDM, Canon ANELVA Corp.) and converted to the permeation flux with a calibration factor using a deuterium standard leak. A thermocouple was set at the sample part in contact with the backside of the sample, and the test temperature was 250–550 °C. The inlet pressure of deuterium was set to 20–120 Pa to simulate a partial pressure of tritium in an actual reactor. Since the partial pressure of residual gas in the upstream was relatively high, the deuterium gas was continuously introduced into the upstream with a small pumping rate to keep a constant pressure of deuterium.

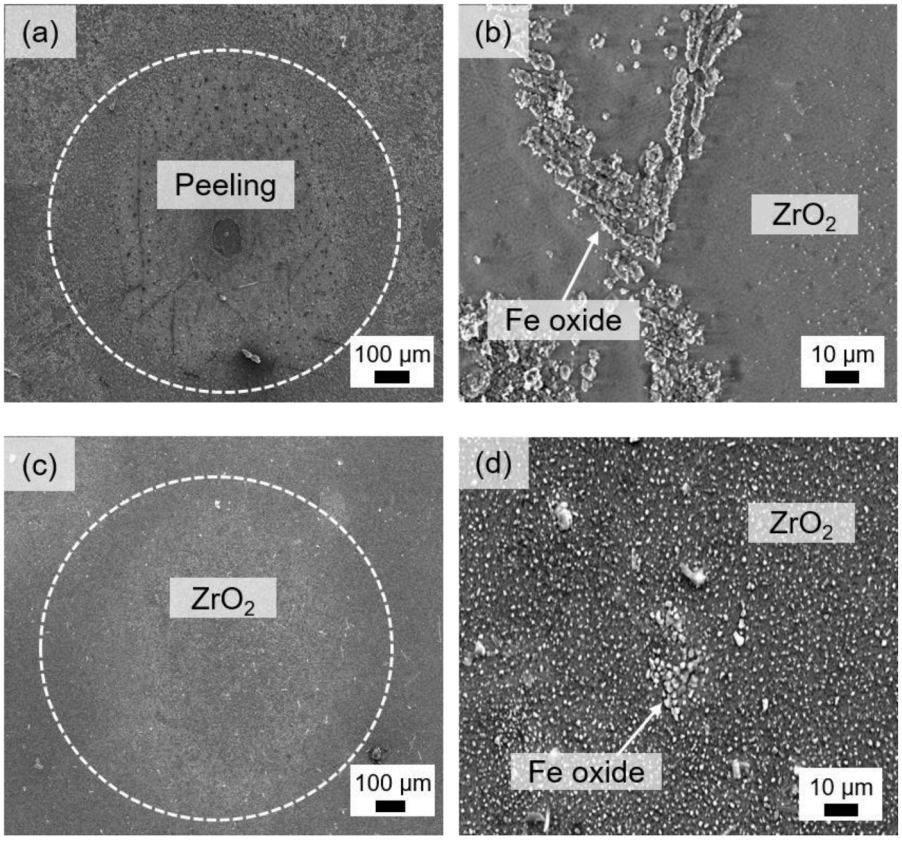

Fig. 1. Surface SEM images of (a) (b) Z30P16 and (c) (d) Z20P16 samples.

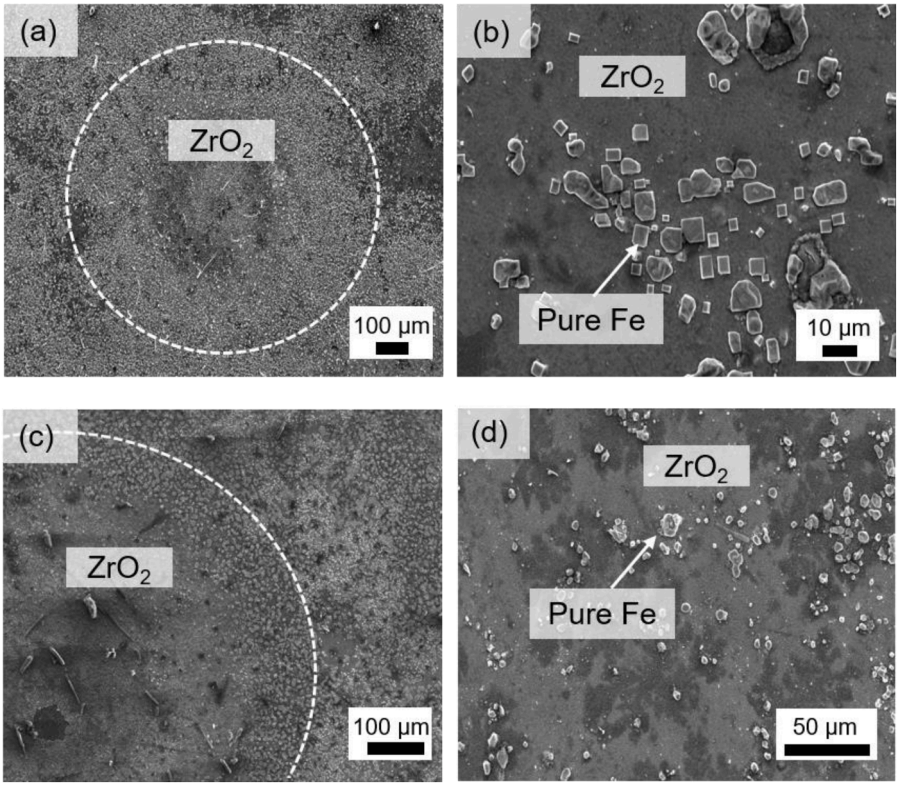

Fig. 2. Surface SEM images of (a,b) Z30P32 and (c,d) Z20P32 samples.

2.4. Characterization

Surface and cross-sectional observations and chemical analyses of the samples were performed by field emission scanning electron microscopy (FE-SEM, JSM-IT700FHR, JEOL Ltd.) with energy dispersive X-ray spectroscopy (EDX). The crystal structure of the samples was analyzed using a grazing incident X-ray diffraction (GIXRD, RINT Ultima III, Rigaku Co. Ltd.). The incident angle was set to 0.5 °.

3. Results and discussion

3.1. Surface analysis

Fig. 1 shows surface SEM images of the Z30P16 and Z20P16 samples. In the pebble-contacting areas indicated as white circles in Fig. 1(a) and (c), zirconium (Zr) was not detected in the Z30P16 sample, indicating the coating stuck to the pebble and peeled off when the pebble was removed, while it was detected in the Z20P16 sample. A partial peeling was only observed in the Z30P16 sample. On the other hand, outside the contacting area the coating remained intact in both samples, as shown in Fig. 1(b) and (d). Iron (Fe) oxides were also formed, as in our previous study [4]. These results indicate that oxygen from H_2O and/or lithium hydroxide (LiOH) was released from the pebbles, passed through the coatings, and reacted with the substrate. Fig. 2 shows surface SEM images of the Z30P32 and Z20P32 samples. In both samples, Fe-oxides including chromium (Cr) were detected, and Zr was not detected in the pebble-contacting area, that is shown in Fig. 2(a) and (c). It is clear that the pebble exposure caused Fe-oxide formation, resulting in the peeling of the coatings, as also indicated our previous study [4]. Outside the contacting area shown in Fig. 2(b) and (d), pure Fe grains were formed, and Zr was detected, suggesting that the Fe-oxides were reduced by hydrogen in the purge gas during the pebble exposure tests.

Fig. 3 shows cross-sectional images and elemental mappings for the Z30P16, Z20P16, Z30P32, and Z20P32 samples. A corrosion layer formed but was peeled off during the fabrication process of the cross-sections. The thickness of the corrosion layer of Z30P16 was 1.8–2.3 μm, which was thicker than that of the Z20P16 sample (~0.25 μm), indicating that the corrosion behavior varied with the pebble composition. On the surfaces of the Z30P32 and Z20P32 samples, the corrosion layer did not occur, while pure Fe and Fe-oxides were formed on the surface. From EDX mappings, the signal of Cr looks overlapping that of Zr, but the fact is that an Fe-Cr-O layer formed beneath the ZrO_2 coating during the MOD process [9]. The Fe-Cr-O layer in the Z30P32 sample was thicker than that in the Z20P32 sample. These results suggest that the higher content of LMT in the breeder pebbles induced the growth of corrosion layers after the annealing tests for both 16 and 32 days.

Fig. 4(a) and (b) show XRD patterns of the samples annealed for 16 days. In addition to the peaks of Fe-oxides, those of ternary oxides containing lithium (Li) were identified in both samples, indicating the diffusion of Li from the pebbles and the reaction with the Fe-oxides. The relative intensity of ZrO_2 to α-Fe in the Z20P16 sample was stronger than that of the Z30P16, suggesting that the coating remained within a larger area. Fig. 4(c) and (d) show the XRD patterns of the sample annealed for 32 days. Although peaks of ternary oxides were observed, relative intensity against α-Fe was weak compared to those of the Z30P16 and Z20P16 samples, which verified that the reduction of the Fe-oxides by hydrogen occurred during the exposure tests. Another possibility is that the X-ray was scattered by pure Fe formed on the surface of the coating.

3.2. Deuterium permeation measurements

Fig. 5 shows the Arrhenius plots of the deuterium permeation flux for the unexposed ZrO_2, Z30P16, and Z20P16 samples with a deuterium driving pressure of 120 Pa. The ZrO_2-coated sample without exposure to the solid breeder pebbles decreased the deuterium permeation flux by a factor of 8800 at 400 °C in comparison with the uncoated F82H substrate. In the following measurements at higher temperatures, however, the permeation reduction performance degraded slightly, which indicates partial cracking of the coating [9]. Both exposed samples show two orders of magnitude higher permeation flux than the unexposed

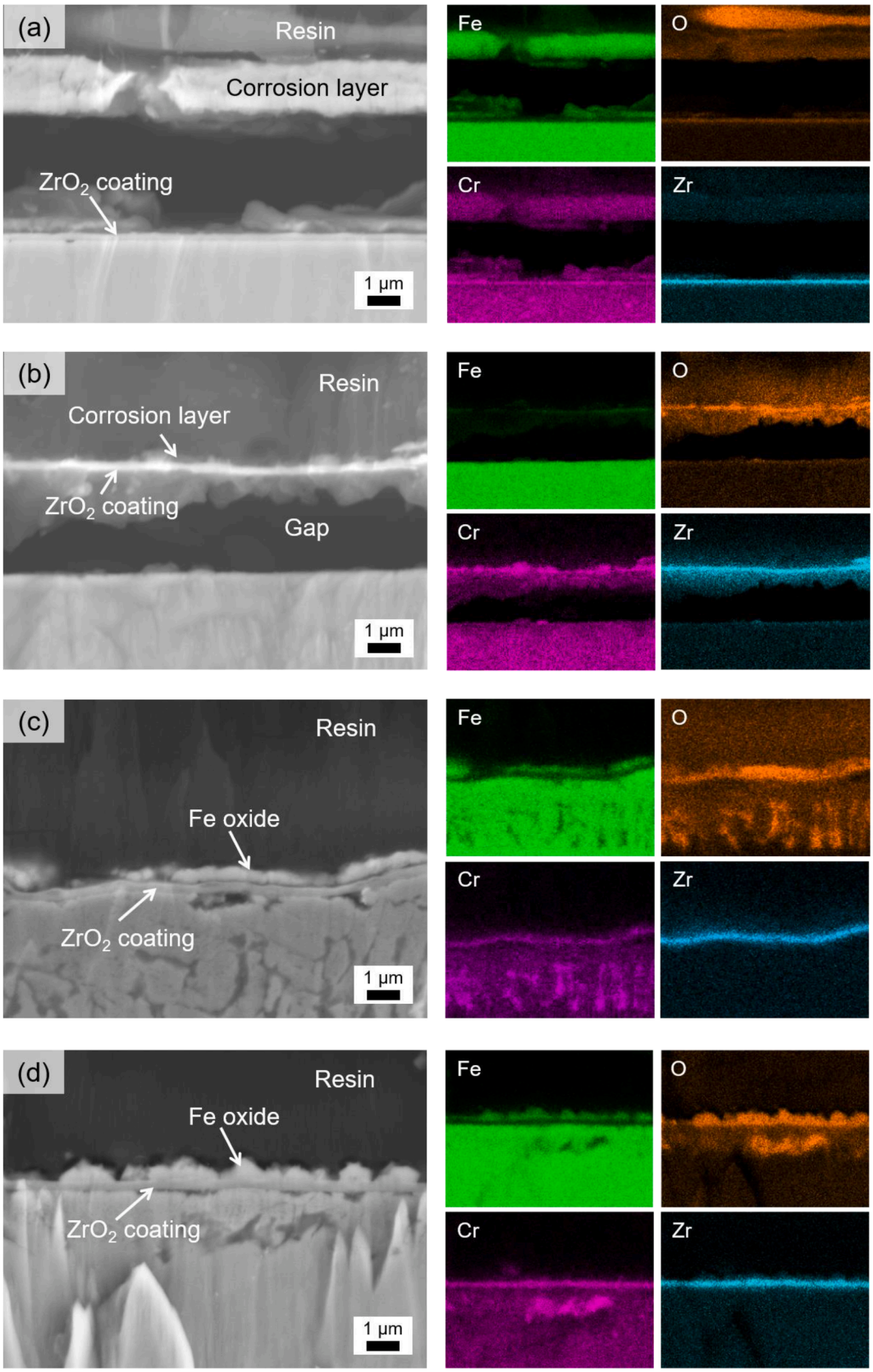

Fig. 3. Cross-sectional images and elemental mappings of (a) Z30P16, (b) Z20P16, (c) Z30P32, and (d) Z20P32 samples.

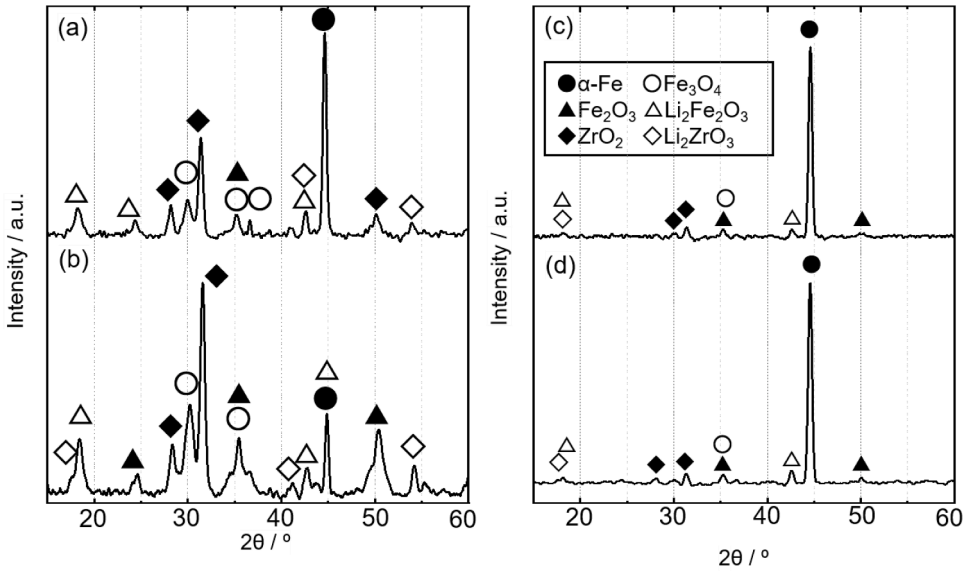

Fig. 4. XRD spectra of (a) Z30P16, (b) Z20P16, (c) Z30P32, and (d) Z20P32 samples.

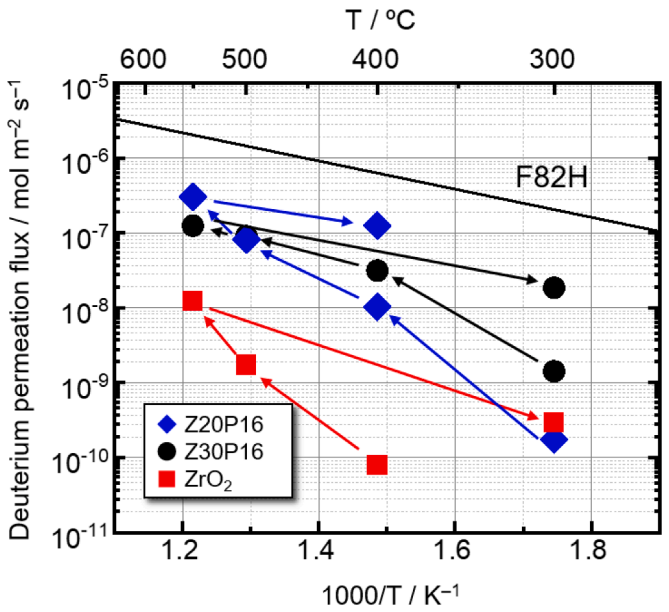

Fig. 5. Arrhenius plots of deuterium permeation flux for unexposed ZrO_2, Z30P16, and Z20P16 samples.

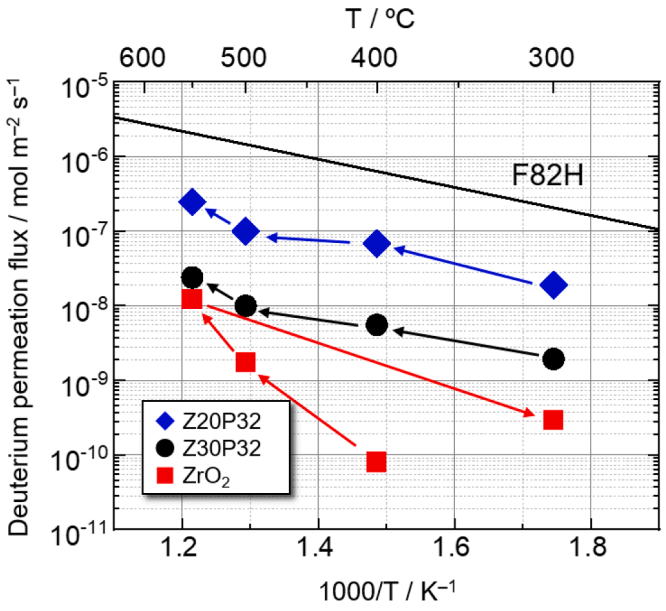

Fig. 6. Arrhenius plots of deuterium permeation flux for unexposed ZrO_2, Z30P32, and Z20P32 samples.

sample at 400 °C, which indicates the degradation of the ZrO_2 layer. According to the surface coverage model [10], we estimated a more than 10% decrease in the surface coverage of the coating. The Z30P16 sample shows permeation fluxes two orders of magnitude lower in comparison with unexposed F82H substrate below 300 °C. The permeation flux increased by an order of magnitude in the measurement at 400 °C and then increased linearly with inverse temperature up to 550 °C. The permeation flux from 400 °C to 550 °C and in the second measurement at 300 °C was an order of magnitude lower than that of the substrate. The corrosion layer decreased the permeation flux at low temperatures; however, a change in the structure of the corrosion layer occurred above 400 °C, leading to the degradation of the permeation reduction performance of the sample. The Z20P16 sample further decreased the permeation flux by one order of magnitude compared to that of the Z30P16 sample at 300 °C, most probably because the coating coverage was higher. However, the permeation flux increased with temperature to the same levels as in the Z30P16 sample and was an order of magnitude lower than that of the substrate at 550 °C. It is assumed that crack formation in the coating occurred during the permeation measurements due to the growth of Fe-oxides.

Fig. 6 shows the results of the permeation measurements for the Z30P32 and Z20P32 samples. The Z30P32 sample shows permeation fluxes two orders of magnitude lower in comparison with those of the substrate in the entire temperature range. The thickness of the corrosion layer increased with the exposure duration, which suppressed the change in the corrosion layer, resulting in a lower permeation flux. The permeation flux of Z20P32 was an order of magnitude lower than that of the substrate. Considering the results of SEM observation and XRD, the coating would degrade unlike in the case of the Z20P16 sample. Therefore, this high permeation flux could be due to the lower thickness of the corrosion layer compared to the Z30P32 sample. Although the ZrO_2 coatings deteriorated during each solid breeder pebbles exposure

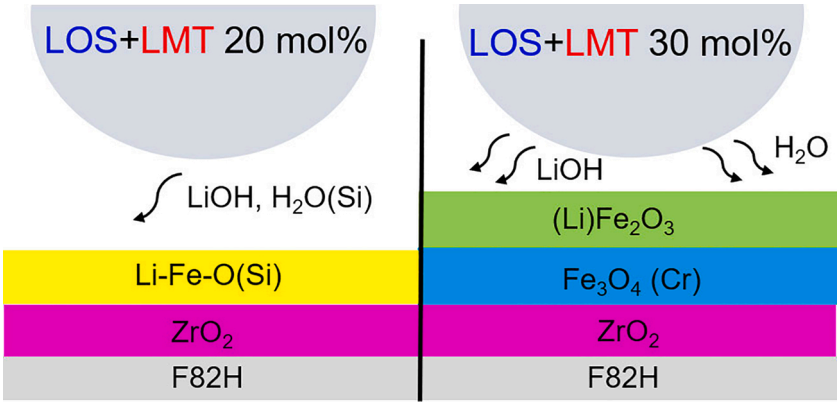

Fig. 7. Conceptual diagram of corrosion mechanism by LOS and LMT phases.

test, the effect of the corrosion products was different depending on the composition of the breeders.

The corrosion mechanism by the different breeder phases can be considered as shown in Fig. 7. Li_2TiO_3 is more corrosive to the substrates than Li_4SiO_4 because Li in Li_2TiO_3 is easier to diffuse [11,12]. Besides, the thickness of the corrosion layer caused by LMT pebbles increases with the exposure time. On the other hand, Li and possibly silicon (Si) released from Li_4SiO_4 phase formed a corrosion layer. However, the thickness of the corrosion layer by the Li_4SiO_4 pebbles did not increase as much as by the Li_2TiO_3 pebbles because Li diffused less in the ceramic pebbles due to a lower content of LMT. Also, a dense vitreous corrosion layer containing Si might work as a protective layer, preventing further corrosion [13,14]. From the above, we consider that the samples exposed to the pebbles with a larger LMT/LOS ratio (LMT30) formed the thicker corrosion layer, resulting in a larger suppression of deuterium permeation. On the other hand, the pebbles with a lower LMT/LOS ratio (LMT20) are less likely to grow the corrosion layer on the sample, leading to a lower permeation reduction performance. To modify the integrity of the coating, a coating with a larger thickness and/or a multilayer structure to suppress diffusion of Li and O is necessary.

4. Conclusions

Deuterium permeation measurements for ZrO_2 coatings fabricated by metal organic decomposition were conducted after annealing with biphasic LOS-LMT pebbles to elucidate the effect of corrosion by the pebbles on the deuterium permeation behavior. The coating after annealing for 32 days shows peeling in the pebble-contacting area, while the coating after annealing for 16 days with 20 mol% LMT pebbles does not. The deuterium permeation flux of the coating after annealing for 32 days with 30 mol% LMT pebbles is an order of magnitude lower than that after annealing for 16 days. In the case of the samples after annealing with 20 mol% LMT pebbles, the permeation flux shows similar values regardless of the annealing duration. The permeation flux of the sample after annealing for 32 days with 30 mol% LMT pebbles is an order of magnitude lower than that with 20 mol% LMT pebbles, suggesting that the composition of the pebble affects the deuterium permeation behavior. In particular, the thickness of the corrosion layer formed on the samples after annealing is probably influenced by the pebble compositions. The 30 mol% LMT pebbles formed the thicker corrosion layer, resulting in a larger permeation reduction, while the corrosion layer formed by the 20 mol% LMT is thinner. Not only the ZrO_2 coating but also the corrosion layer affects the tritium permeation behavior in the solid breeder blankets.

Declaration of Competing Interest

The authors declare that they have no known competing financial interests or personal relationships that could have appeared to influence the work reported in this paper.

Data availability

Data will be made available on request.

Acknowledgments

This work was supported by JSPS KAKENHI Grant Number 19H01873.

References

[1] G.W. Hollenberg, et al., Tritium/hydrogen barrier development, Fusion Eng. Des. 28 (1995) 190–208.
[2] J. Konvs, et al., Status of tritium permeation barrier development in the EU, Fusion Sci. Technol. 47 (2005) 844–850.
[3] T. Chikada, R. Konings, R. Stoller, et al., Ceramic coatings for fusion reactors, in: Comprehensive Nuclear Materials, 2nd edition, 6, Elsevier, Oxford, 2020, pp. 274–283.
[4] T. Chikada, et al., Compatibility of tritium permeation barrier coatings with ceramics pebbles, Corros. Sci. 182 (2021), 109288.
[5] J. Mochizuki, et al., Preparation and characterization of Er_2O_3-ZrO_2 multi-layer coating for tritium permeation barrier by metal organic decomposition, Fusion Eng. Des 136 (2018) 219–222.
[6] R. Knitter, et al., Fabrication of modified lithium orthosilicate pebble by addition of titania, J. Nucl. Mater. 442 (2013) S433–S436.
[7] J.M. Heuser, et al., Long-term thermal stability of two-phase lithium orthosilicate metatitanate ceramics, J. Nucl. Mater. 507 (2018) 396–402.
[8] T. Chikada, et al., Deuterium permeation behavior of erbium oxide and coating on austenitic, ferritic, and ferritic/martensitic steels, Fusion. Eng. Des. 84 (2009) 590–592.
[9] T. Chikada, et al., Deuterium permeation through erbium oxide coatings on RAFM steels by a dip-coating technique, J. Nucl. Mater. 442 (2013) 533–537.
[10] T. Chikada, et al., Modeling of tritium permeation through erbium oxide coatings, Fusion Sci. Technol. 60 (2011) 389–393.
[11] H. Kashimura, et al., Mass loss of Li_2TiO_3 pebbles and Li_4SiO_4 pebbles, Fusion Eng. Des. 88 (2013) 2202–2205.
[12] K. Mukai, et al., Lithium vapor of hyper-stoichiometric lithium metatitanate $Li_{2.13}$ $_{(2)}TiO_{3+y}$, J. Phys. Chem. 124 (2020) 10872–10877.
[13] T. Hernandez, et al., Corrosion mechanism of Eurofer produced by lithium ceramics under fusion relevant conditions, Nucl. Mater. Energy 15 (2018) 110–114.
[14] I.W. Donald, Preparation, properties and chemistry of glass and glass-ceramic-to-metal seals and coating, J. Mater. Sci. 28 (1993) 2841–2886.